

## ***Final Report***

<b><i>Titolo del programma:</i></b>	Synthesis, structural and morphological characterization of hollow spinel ferrite nanoparticles.
<b><i>Proponente:</i></b>	Elisabetta Agostinelli
<b><i>Fruitore:</i></b>	Davide Peddis
<b><i>Istituto di afferenza del Fruitore:</i></b>	Istituto di Struttura della Materia
<b><i>Istituzione ospitante:</i></b>	Norwegian University of Science and Technology (NTNU) Nanolab, Norway
<b><i>Periodo di Parmanenza:</i></b>	21 Giugno, - 14 Luglio

### **1. Introduction**

Spinel ferritic oxides nanoparticles (NPs) with a non-collinear spin structure (spin-canting) at the surface have attracted a great interest both for applications and for basic research. Interface exchange coupling between a magnetically ordered core and a magnetically disordered shell with high anisotropy may occur, inducing interesting magnetic properties. From this point of view, hollow NPs composed of randomly oriented grains clumped together are very interesting because both inner and outer surfaces of the hollow NP contribute to the total surface, leading to very high surface anisotropy and strong spin-canting. In addition hollow NPs have many potential applications, such as magnetic drug delivery, cosmetics, inks, catalysis, piezoelectric converters and sound insulators of low dielectric constant because of the remarkably high surface area associated with them<sup>1,2</sup>. As a further improvement of this material, coating hollow ferrimagnetic (Fi) NPs with antiferromagnetic (AF) shell opens new and interesting perspectives for technological uses of these materials. In fact, the F/AF exchange interactions give rise to an additional anisotropy which affects the magnetization reversal process of the whole system, producing significant changes in the coercivity (exchange bias, EB)<sup>3,4</sup>. During the period at the NTNU the activity of Davide Peddis (DP) was mainly devoted to the synthesis of different iron oxide hollow nano-architectures. In particular different lines has been followed:

- a) Synthesis of iron oxide hollow nanoparticles (HN) [section 4]
- b) Preparation of iron oxide nano-container [section 4.1]
- c) Synthesis of hollow iron oxide nanoparticles coated with a shell of antiferromagnetic oxides (NiO, MnO) [section 5].

During the stay of DP in NTNU more than 20 synthesis have been performed and most of the data (TEM images, XRD spectra) are still under elaboration. In this report, only the most significant results will be discussed.

The first step for the preparation of all the systems under investigation during this project has been the synthesis of iron/iron oxide nanoparticles, based on thermal decomposition of iron pentacarbonyl (section 3)<sup>5</sup>.

## 2. Experimental

X-Ray Diffraction (XRD) analysis were done using a Bruker D8 ADVANCE with DAVINCI design diffractometer, with Cu-K $\alpha$  wavelength. For TEM observations, the samples powders were dispersed in hexane, then the suspensions were dropped on carbon-coated copper grids and observed using a Hitachi S-5500 scanning transmission electron microscope (S-TEM). TEM images were processed and analysed with “*image J*” software<sup>6</sup>.

## 3. Iron/iron oxide nanoparticles.

The synthesis of iron/iron oxide NPs was carried out by using commercially available chemicals. In a double neck flask, a mixture ODE (25 mL) and ligand was stirred magnetically and degassed under Ar atmosphere at 120°C for 30 min. The temperature of the reaction mixture was raised to 180°C before injecting Fe(CO)<sub>5</sub> (1.4 mL, 10.36 mmol) to the hot solution under Ar atmosphere. The time for changing the colour from orange to brown and finally to black depends on the surfactant type used during the reaction. In the case of OA and HDA, immediate change of colour (~2 min) was observed while a gradual change in colour from orange to black was observed after approx. 10 min. After 30 min of reaction at 180°C, the temperature was quickly raised to 220°C for 120 min. The supernatant was decanted after cooling down the solution to room temperature, and magnetic stir bar coated with magnetic NPs was washed with hexane. The solution was precipitated out by adding acetone, and redispersed in hexane. By varying synthesis parameters (e.g. molar ratio of the surfactant) the NPs size was modulated in the range 5 – 20 nm in order to change the surface/volume ratio<sup>5</sup>. The structural characterization (X-ray diffraction, High Resolution TEM) clearly indicated that both core and shell are amorphous<sup>7</sup>. As an example, TEM images of iron/iron oxide amorphous core shell particles are reported in figure 1 a-b.

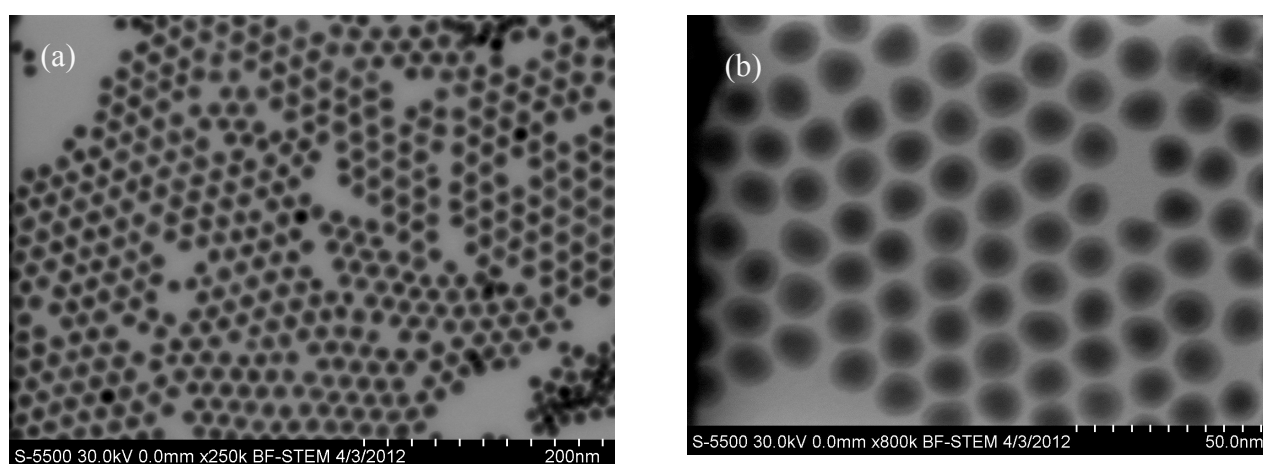


Figure 1a-b: TEM images of iron/iron oxide nanoparticles

#### 4. Hollow iron oxide nanoparticles

By a controlled oxidation of iron/iron oxide nanoparticles the so-called Kirkendall effect (i.e.: different diffusion rates of metal ions) is induced leading to the formation of iron spinel oxides ( $\text{Fe}_3\text{O}_4$ ,  $\gamma\text{-Fe}_2\text{O}_3$ ) hollow NPs nanoparticles. The novelty of this synthetic approach is that 1,2 hexadecane diol (HDD) has been used as oxidizing agent for the first time. In a typical synthesis 100 mg of Fe/FeO NPs, 100 mg of HDD, 250  $\mu\text{l}$  of Oleylamine (OLY) and 25 ml of Octadecene (ODE), have been mixed in a triple neck flask under vigorous magnetic stirring (1000 rpm). The temperature of the reaction mixture was raised by an oil under Ar atmosphere at  $210^\circ\text{C}$  and after 240 min the system was cooled down to room temperature. Then the particles were precipitated out by adding acetone, and redispersed in hexane.

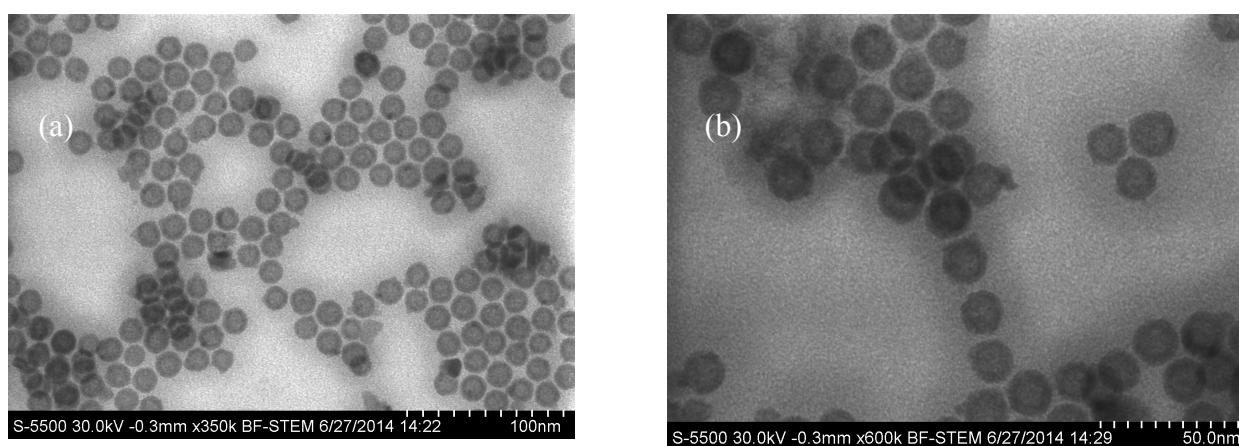


Figure 2 a b: TEM images of iron oxide hollow nanoparticles

TEM images (Figure 2a-b ) clearly indicate the formation of hollow nanostructures. A detailed statistical analysis has been done on TEM images, measuring the total diameter ( $D$ , inset Figure 3) and the inner diameter ( $D_i$ , inset Figure 3) of the hollow particles.

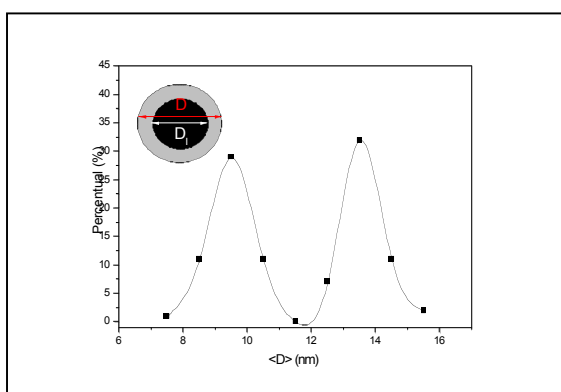


Figure 3: Distribution of the total and inner diameter ( $D$  and  $D_i$ , inset Figure 3) of the hollow nanoparticles obtained by statistical analysis of TEM images.

Hollow iron oxide nanoparticles have an inner-to-total diameter ratio of  $D_1 / D \approx 0.7$  and relatively narrow particle-size distributions. The mean total diameter of the particles is around 14 nm, with a shell thickness around 2 nm. Changing the size of Fe/FeO nanoparticles it was possible to obtain hollow iron oxide nanoparticles with different size.

#### 4.1 Iron oxide .Nano-container.

Several experiments have been done in order to study the oxidation process, using mainly two approaches:

A) Keeping fixed the reaction time experiment (240 min) experiments were done using different amount of HDD (50 mg – 2 g).

B) Keeping fixed the amount of HDD, the kinetic of reaction was studied doing TEM analysis after different reaction time (15 min – 1700 min).

Very exciting results have been obtained using a low quantity of HDD (50 mg) and very long reaction time (about 1500 min). In these conditions a local degradation of the iron oxide shell was observed, leading to formation of “nano-container” with the morphology shown in the TEM images reported in Figure 4a-d.

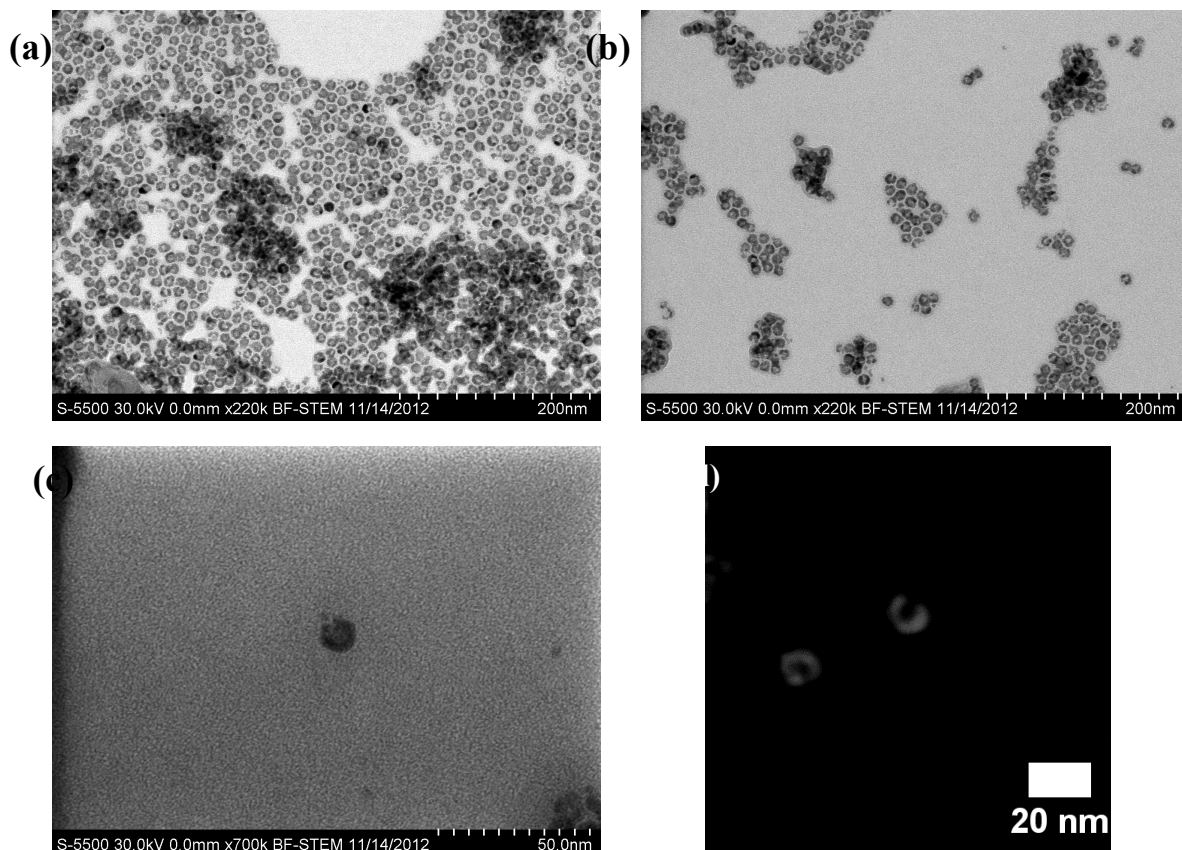


Figure 4: TEM images of “nano-container”

## 5. Ferrimagnetic/antiferromagnetic shell-shell nanoparticles

As a further tool to tune the magnetic anisotropy of hollow nanoparticles, a synthetic approach was developed to deposit a shell of antiferromagnetic materials (NiO, MnO) onto the surface of the hollow structure. In this way, hollow shell-shell nanoparticles (HNSS) were obtained. The novelty of the adopted synthetic strategy is to induce, at the same time, the oxidation of iron/iron oxide nanoparticle, leading to the hollow structure, and the deposition of a thin layer of antiferromagnetic oxide on the surface. In a typical synthesis the procedure described in section 4 is used. The difference is that also 0.5 mol of Manganese acetylacetonate [Mn(acac)] and Ni acetylacetonate, [Ni(acac)] were also added in the initial mixture to obtain a shell of NiO and MnO, respectively. As an example TEM micrographs of iron oxide/nickel oxide HNSS are reported in Figure 5.

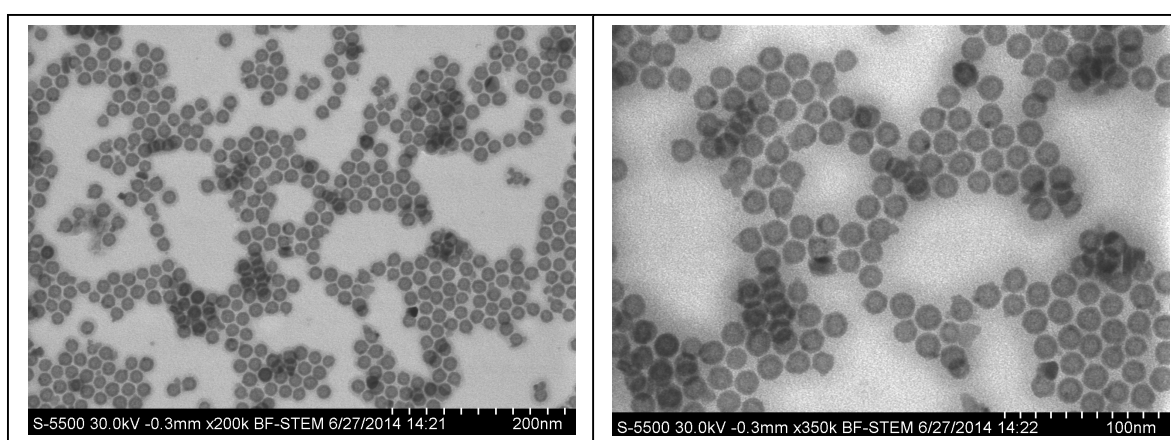


Figure 5: TEM images of iron oxide/nickel oxide HNSS.

Chemical analysis (not reported here) clearly indicated the presence of Ni, Fe and O in the sample. In order to verify the formation of NiO shell, a statistical analysis was performed on TEM images. The distribution of  $D$  and  $D_i$  of two samples of iron oxide HN (figure 6a) and iron oxide/nickel oxide HNSS are reported in Figure 6b.

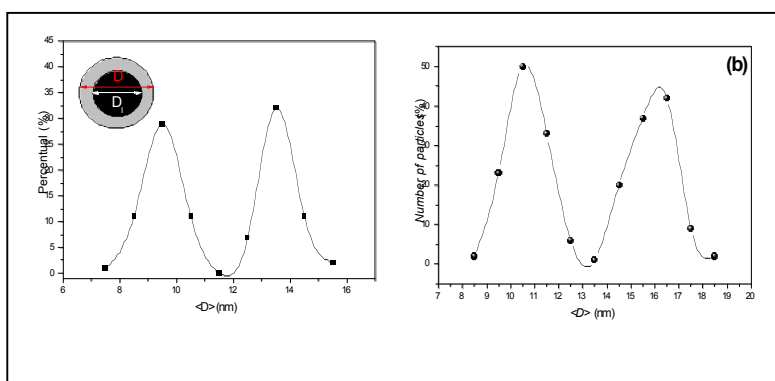


Figure 6: Distribution of the total diameter ( $D$ ) and the inner diameter ( $D_i$ ) of HN (a) and HNSS (b) obtained by statistical analysis of TEM images.

The inner diameter is almost the same in both samples, while the total diameter increases from ~14 nm in HN sample to ~ 16 nm in HNSS sample. This means an increase of the shell thickness of about 1 nm, which is compatible with the formation of a NiO shell.

Using the same synthetic approach, interesting results were also obtained using iron-acetylacetonate [Fe(acac)] to obtain nanoparticles with different shell thickness.

1. H.J. Fan, U. Gösele, and M. Zacharias. *Formation of Nanotubes and Hollow Nanoparticles Based on Kirkendall and Diffusion Processes: A Review. Small* **3**, 1660–1671 (2007).
2. A. Cabot, V.F. Puentes, E. Shevchenko, Y. Yin, L. Balcells, M.A. Marcus, S.M. Hughes, and A.P. Alivisatos. *Vacancy Coalescence during Oxidation of Iron Nanoparticles. J. Am. Chem. Soc.* **129**, 10358–10360 (2007).
3. J. Nogués, and I.K. Schuller. *Exchange Bias. J. Magn. Magn. Mater.* **192**, 203–232 (1999).
4. J. Nogués, J. Sort, V. Langlais, V. Skumryev, S. Suriñach, J.S. Muñoz, and M.D. Baró. *Exchange Bias in Nanostructures. Phys. Rep.* **422**, 65–117 (2005).
5. G. Singh, P.A. Kumar, C. Lundgren, A.T.J. van Helvoort, R. Mathieu, E. Wahlström, and W.R. Glomm. *Tunability in Crystallinity and Magnetic Properties of Core-Shell Fe Nanoparticles. Part. Part. Syst. Charact.* n/a–n/a (2014). doi:10.1002/ppsc.201400032
6. J. Schindelin, I. Arganda-Carreras, E. Frise, V. Kaynig, M. Longair, T. Pietzsch, S. Preibisch, C. Rueden, S. Saalfeld, B. Schmid, J.-Y. Tinevez, D.J. White, V. Hartenstein, K. Eliceiri, P. Tomancak, and A. Cardona. *Fiji: An Open-Source Platform for Biological-Image Analysis. Nat. Mater.* **9**, 676–682 (2012).
7. P.A. Kumar, G. Singh, W.R. Glomm, D. Peddis, E. Wahlström, and R. Mathieu. *Superspin Glass State and Exchange Bias in Amorphous Fe/Fe-O core/shell Nanoparticles. Mater. Res. Express* **1**, 036103 (2014).

*André P. Glomm*

Roma, September 12, 2014

